Supporting Information

Absorption of Light in a Single-Nanowire Silicon Solar Cell Decorated with an Octahedral Silver Nanocrystal

Sarah Brittman,[1,2]*† Hanwei Gao,*[1,2]*† Erik C. Garnett,*[3] *and Peidong Yang*[1,2]***

† These authors contributed equally to this work.

[1]Department of Chemistry, University of California, Berkeley, California 94720, United States

[2]Materials Science Division, Lawrence Berkeley National Laboratory, 1 Cyclotron Road, Berkeley, California 94720, United States

[3]Department of Materials Science and Engineering, Stanford University, Stanford, California 94305, United States

* Please address correspondence to p_yang@berkeley.edu.

Fabrication of the suspended single-nanowire solar cells

Trench substrates were fabricated from heavily doped ($\rho < 0.01\ \Omega$ cm), p-type (boron) silicon-on-insulator with a 5 μm device layer oriented <110> and 500 nm buried oxide layer (Ultrasil Corp.). The device layer was etched to ~2.2 μm using anisotropic plasma etching with SF_6 (Surface Technology Systems). Then 8-μm-wide trenches were patterned with photolithography and anisotropically etched into the device layer to the buried oxide. Photoresist was removed in PRS-3000 heated to 85°C and piranha solution heated to 120°C.

Silicon nanowires were grown bridging the trenches via the vapor-liquid-solid (VLS) mechanism using 250-nm Au catalyst particles. Prior to growth, the trench substrates were etched in 10:1 buffered hydrofluoric acid (BHF) for 10 seconds. 10% aminopropyl-trimethoxysilane or 10% aminopropyl-triethoxysilane in ethanol was used as a linking molecule for the 250-nm Au colloids (Ted Pella, Inc.) drop cast onto the substrates. Silicon nanowires were grown at 850°C using $SiCl_4$ as a precursor and 10% hydrogen in argon in a home-built, chemical vapor deposition (CVD) system consisting of a quartz tube in a tube furnace. Reactions to grow wires bridging the trenches lasted from 15 to 45 mins.

After growth the nanowires were p-doped with boron. Prior to doping, the nanowires were etched for ~30 seconds in 10:1 BHF and soaked in I_3/KI gold etchant (Transene) for at least 20 minutes. The nanowires were then p-doped in a tube furnace using 1% BCl_3 in argon and 10% hydrogen in argon at 800°C. For the first hour, 1 sccm of dilute BCl_3 with 100 sccm of hydrogen/argon was used, followed by a two-hour anneal in 50 sccm of hydrogen/argon and no BCl_3. Assuming uniform radial doping, the doping concentration was estimated to be ~10^{17} cm^{-3} based on the resistivity approximated from two-point electrical measurements and geometric estimates from the scanning electron microscopy (SEM) images.

After p-doping, the nanowires underwent an additional gold etch and were then coated in ~400 nm of silicon dioxide deposited using plasma enhanced chemical vapor deposition (PECVD) using silane and nitrous oxide precursors at 350°C (Oxford Corp.). Oxide-coated trench substrates were then exposed to hexamethyldisilazine (HMDS) vapor before coating in photoresist and lithographically exposing the bridging nanowire's left contact and a portion of the nanowire. The exposed oxide was etched in 5:1 BHF for 2 to 2.5 minutes, and the photoresist was removed by soaking for over an hour in PRS-3000 (Baker) heated to 85°C.

The nanowires were then annealed at 800°C under rough vacuum for 1.5 hours about 1 mm beneath a silicon substrate coated with P509 phosphorus spin-on dopant (Filmtronics Corp.). After annealing, the oxide mask was removed with 5:1 BHF. The nanowire substrate was then coated with 4 nm aluminum oxide in a home-built atomic layer deposition system using water and trimethyl-aluminum as precursors at 200°C.

Electrical contact was made to the single-nanowire devices by wirebonding aluminum wires from the sides of the trenches to the bonding pads of a dual-inline-pin package.

Optical and electrical measurements

A 150 W xenon arc lamp (Newport Corp.) with an AM 1.5G filter was used to measure the nanowire's photovoltaic response. The light intensity was calibrated using a 1.1 mm x 1.1 mm silicon photodiode referenced to a calibrated silicon photodiode (Newport Corp.). *I-V* characterization was performed with a Keithley 236 source-measure unit (SMU).

A home-built confocal microscope with piezoelectric scanning stage was used for simultaneous reflection imaging and scanning photocurrent mapping (SPCM). A helium-cadmium laser (λ=442 nm) was focused to a diffraction-limited spot through the microscope's objective lens (NA = 0.95), with power density ~7 W/cm^2. At each point in the reflection image, the photocurrent was recorded by a Keithley 236 SMU. Photocurrent maps were plotted using MATLAB®, and the reflection images were processed using *Image SXM*.[1]

The dependence of the photocurrent on wavelength (photocurrent spectrum) was obtained by measuring the current generated in the device at 10-nm increments, normalized by the photon flux of the source. A 300 W xenon arc lamp (Newport Corp.) was coupled to a monochromator (Newport Corp.) to obtain monochromatic illumination. The output of the source was measured using a 1.1 x 1.1 mm silicon photodiode (Hamamatsu Corp.) referenced to a calibrated silicon photodiode (Newport Corp.). For wavelengths below 650 nm, a diffuser made of ground quartz was positioned between the source and device to make the spot more spatially uniform. This provided greater positioning tolerance. The diffuser was removed for wavelengths longer than 650 nm to obtain more light since silicon absorbs poorly at longer wavelengths. To achieve the greatest precision between measurements, devices were positioned using a micrometer driven translation stage (Thorlabs).

Finite-difference time domain simulations (FDTD)

The simulations were carried out using the commercial FDTD software package Lumerical® FDTD Solutions 7.0. The geometries of the nanowire and the nanocrystal were estimated according to the SEM images (Figure 1c), and sharp corners and edges were rounded to reflect the experimental structures. The optical properties (i.e. complex electric permittivities) of the Si and Ag were adapted from the literature (Si from Palik,[2] Ag from Johnson and Christy[3]). To avoid simulation artifacts from the meshing of the thin dielectric layer, a 4-nm air gap was used between the nanowire and the nanocrystal in place of the alumina coating. The simulation volume was 5 μm (x) by 4 μm (y) by 3 μm (z) with periodic boundaries along the x-axis and perfectly matched layer boundaries along the y- and z-axes. A plane wave propagating along the -z direction was used as the excitation source. Convergence tests indicated that a 3-nm grid size in the Si nanowire region was enough to produce converged absorption spectra. The absorption spectra were calculated using a 3D field-profile monitor that recorded the instant electromagnetic field components at each grid point so that the absorption cross-section of the Si nanowire could be distinguished from the absorptive contribution of the Ag nanocrystal.

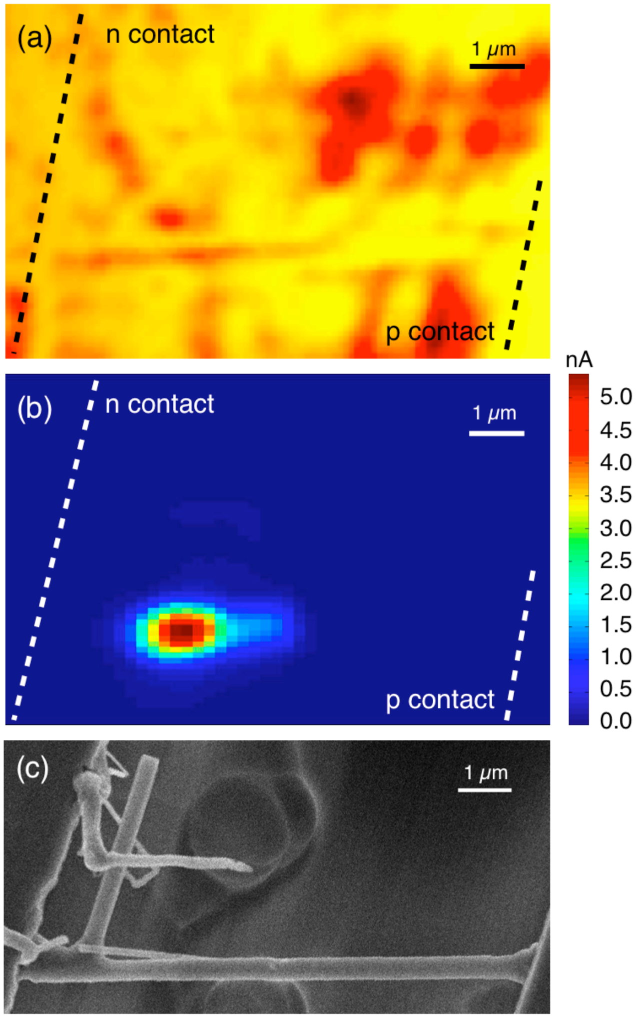

Figure S1. Scanning optical image (a), corresponding scanning photocurrent map (b), and top view SEM image of a single-nanowire solar cell with an axial junction instead of a core-shell junction. The current decays rapidly from the junction on both sides, indicating short minority carrier diffusion lengths (< 1 μm) in both the p- and n-type regions of the nanowire.

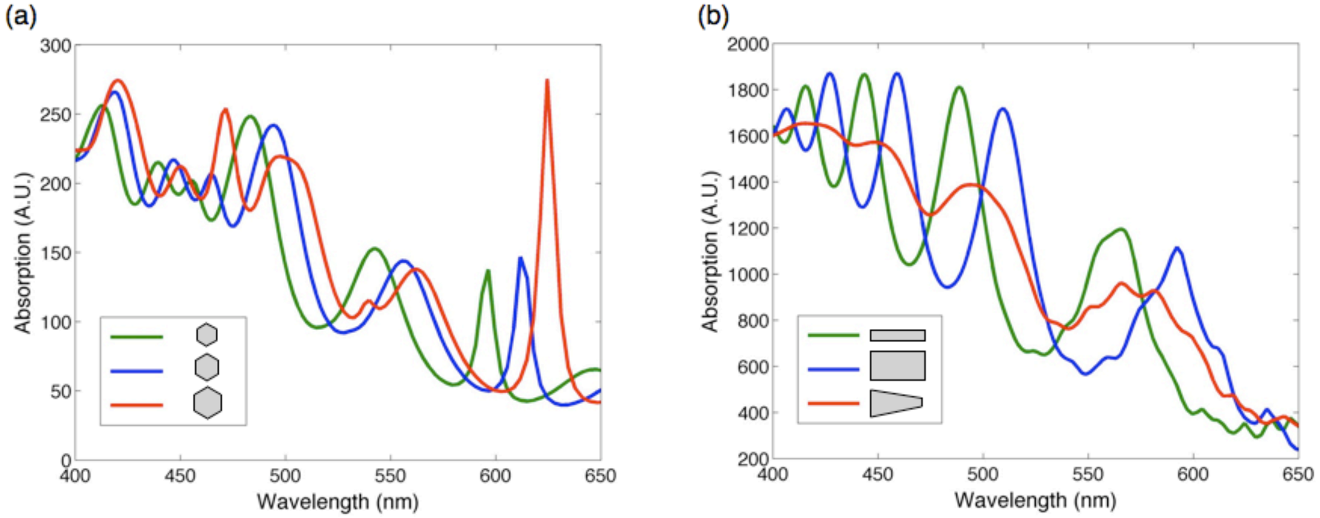

Figure S2. Two-dimensional numerical simulations demonstrating how tapering of a silicon nanostructure broadens the peaks in its absorption spectrum that correspond to its optical resonances. In (a), hexagonal wires of diameters 285 nm, 290 nm, and 295 nm show that the optical resonances red shift with increasing diameter. In (b), a plane of silicon whose thickness tapers from 295 to 285 nm over 4 μm (red curve) shows broadened resonance peaks whose maxima lie between the resonances predicted by the dimensions of either end, 285 nm (green curve) and 295 nm (blue curve). A nanowire tapering from 285 to 295 nm would therefore be expected to exhibit a broadened peak as in (b) but centered at the blue peak positions in (a). It should be noted that (a) is a two-dimensional simulation, so its peaks do not quite match those of the simulation in the main text, which shows a three-dimensional simulation.

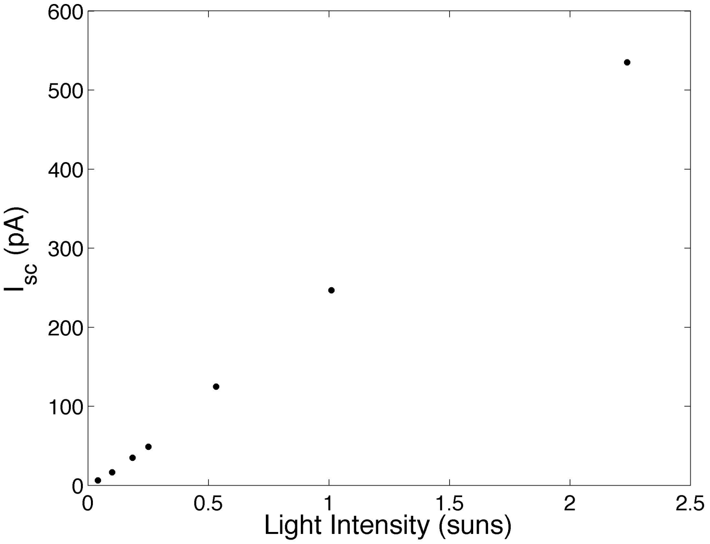

Figure S3. Dependence of the short-circuit current (I_{sc}) on light intensity for a silicon single-nanowire solar cell, showing that the device responds linearly to increasing illumination.

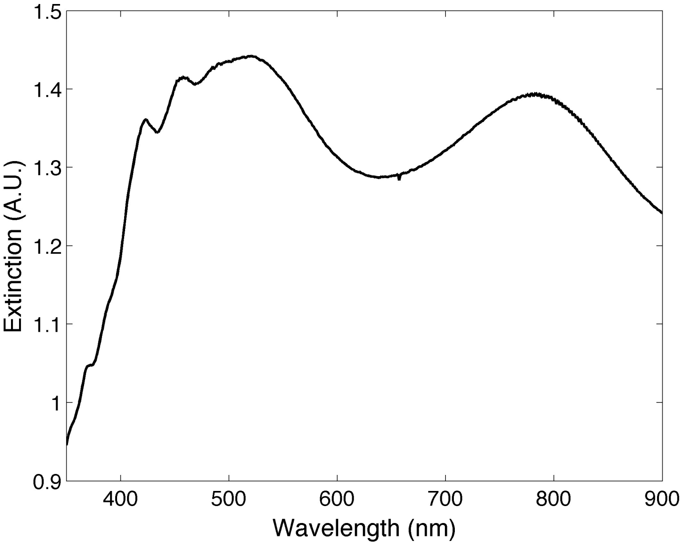

Figure S4. Extinction spectrum of the silver octahedra suspended in ethanol showing the predominantly dipolar (~780 nm) and quadrupolar (~510 nm) peaks.

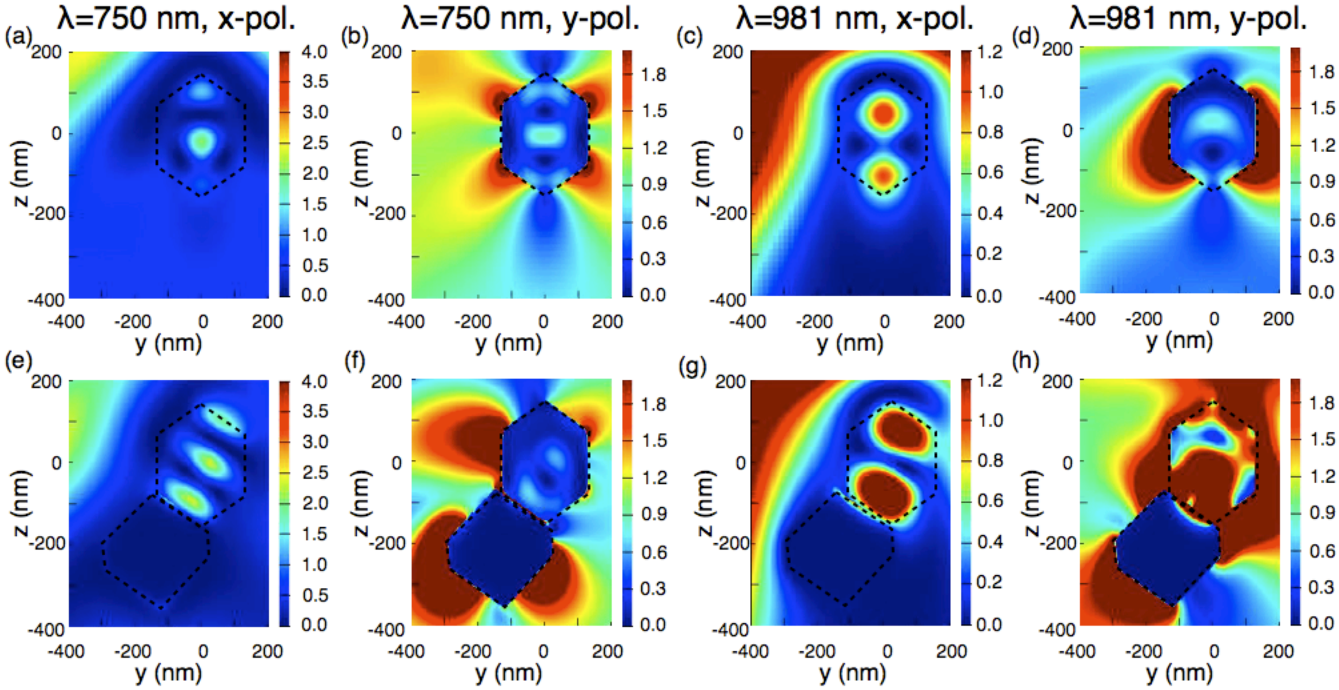

Figure S5. Numerical simulations of the magnitude of the electric field before (a-d) and after (e-h) the addition of the silver octahedron on the wire with a 288 nm diameter. The plots are cross-sections through the center of the nanocrystal, and the wavelengths correspond to the nanocrystal's quadrupolar (750 nm) and dipolar (981 nm) resonances. Both *x*-polarized and *y*-polarized excitations are shown. The particle clearly enhances the field within the wire in all cases except (f). In this case, the field enhancement occurs near the edge of the nanocrystal rather than at its center (plot not shown).

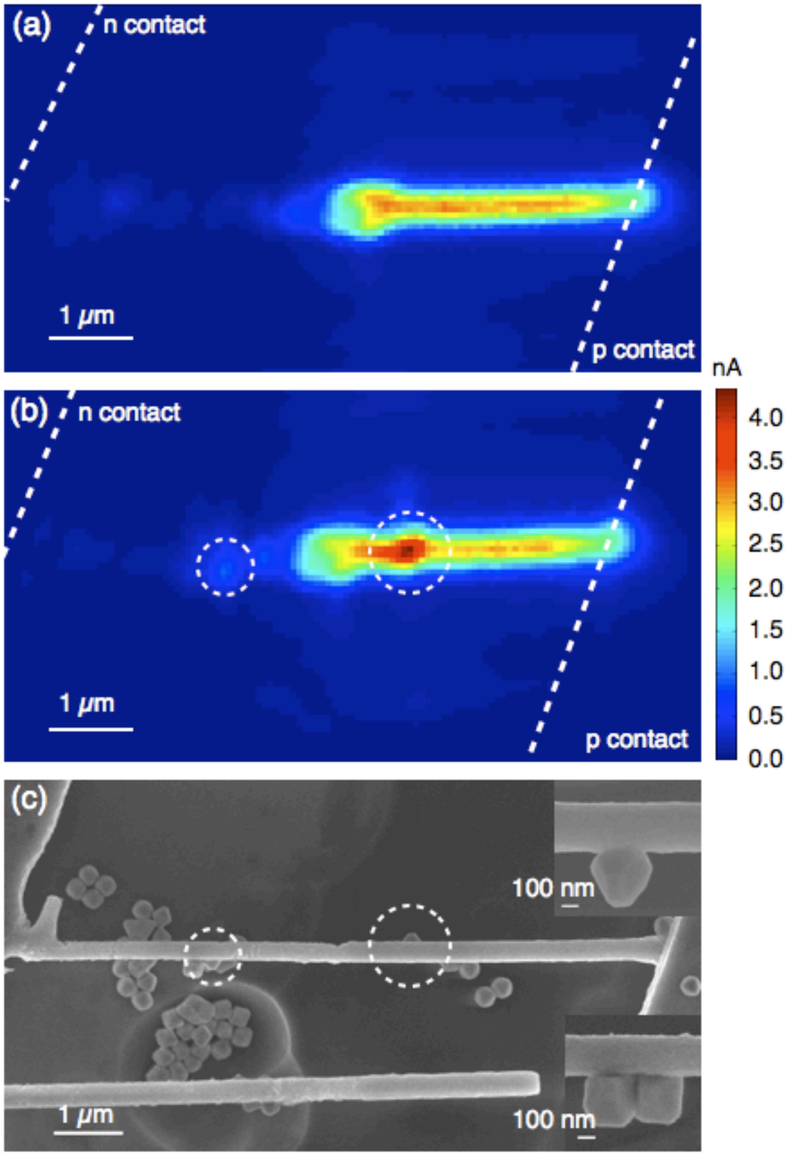

Figure S6. Scanning photocurrent maps of a single-nanowire solar cell (289 nm diameter) before (a) and after (b) the addition of silver octahedra. The larger increase in peak photocurrent (1.3 nA) occurs at the position of the silver octahedron on the active portion of the wire (large circle, top inset in (c)), while a smaller increase (0.8 nA) arises from the far-field scattering of the dimer of octahedra on the inactive portion of the wire (small circle, lower inset in (c)). Both scans show the same device and were taken using a diode laser with λ=650 nm, P~28 W/cm^2. Top view scanning electron microscopy (SEM) image of the same device (c), and insets are side view SEM images of the octahedra attached to the wire.

References

1. Image SXM, S. D. Barrett. http://www.ImageSXM.org.uk. 2008.

2. Palik, E. D., *Handbook of Optical Constants of Solids*. Elsevier: 1998.

3. Johnson, P. B.; Christy, R. W. *Phys. Rev. B* **1972,** 6, 4370-4379.